Earth Science Informatics
https://doi.org/10.1007/s12145-023-01070-z

RESEARCH

# Ionospheric scintillation characteristics over Indian region from latitudinally-aligned geodetic GPS observations

**Sampad Kumar Panda**[1] · **Mefe Moses**[2] · **Kutubuddin Ansari**[3] · **Janusz Walo**[3]

Received: 18 April 2023 / Accepted: 4 August 2023


## Abstract

Ionospheric scintillations pose one of the biggest threats to Satellite-Earth communication links in the communication and navigation systems services whose occurrence characteristics could be explained through the strength of fading (amplitude scintillation index; S4) and the rapidity of the fades (decorrelation time; $\tau 0$). In the present work, we analyzed the S4 index from a latitudinal array of three geodetic global positioning system (GPS) stations along the Indian longitude sector during the descending phase of the 24th solar cycle. The results show predominant occurrences of scintillations during the post-sunset and nighttime periods indicating the level of scintillations close to equatorial, beyond anomaly crest, and near mid-latitude locations. The strong amplitude scintillations during 2014 and 2015 and their lowest magnitudes during 2016 and 2017 reflect the solar activity dependence of the scintillation occurrences. The directional distribution and 2-dimensional surface sky plots of the S4 index substantiate the occurrence of intense scintillation being more prevalent towards the equatorial location, whereas the weak and moderate scintillations are perceived towards the higher low latitude stations. The occurrences of intense scintillations are confirmed in high solar active years and equinox season at all stations, while the equatorial station presents relatively higher occurrences in winter followed by summer. The summer season witnessed intense occurrences even under moderate to low solar activity years (2016–2017), reflecting the post-midnight occurrences due to meridional thermospheric winds. Moreover, maximum percentage occurrences of weak scintillations in all seasons are evident towards the poleward side, far away from the anomaly crest. The amplitude scintillation frequency during the period is further compared with the solar and geomagnetic indices to substantiate the analysis drawn from the variations. The correlation coefficients between the scintillation index occurrence rate with the solar and geomagnetic in-dices at three GNSS stations provide valuable insights into the relationship between solar activity and scintillation. The results show that the strength and direction of the correlation can vary significantly depending on the specific solar index and location. Thus, emphasize further studies on scintillation occurrences for developing effective forecasting and mitigation models over the Indian low-latitude region.

**Keywords** Global positioning system · Amplitude scintillation · S4 index · Equatorial Ionosphere · Indian longitudes

Communicated by H. Babaie.

✉ Sampad Kumar Panda
sampadpanda@gmail.com; sampadpanda@kluniversity.in

Mefe Moses
mmoses@abu.edu.ng

Kutubuddin Ansari
kdansarix@gmail.com

Janusz Walo
j.walo@gik.pw.edu.pl

[1] Department of ECE, Koneru Lakshmaiah Education Foundation, Guntur, Andhra Pradesh 522301, India

[2] Department of Geomatics, Ahmadu Bello University, Zaria, Kaduna 810282, Nigeria

[3] Faculty of Geodesy and Cartography, Warsaw University of Technology, Warsaw, Poland

Published online: 09 August 2023

## Introduction

Ionospheric plasma irregularities can be observed in the form of equatorial plasma bubbles (EPBs) or plasma density depletion in situ satellite and rocket measurements, equatorial spread F (ESF) in ionograms, bite-outs in airglow images, plumes in coherent very high frequency (VHF) backscatter radar, patches in incoherent scatter radar (ISR) measurements, and scintillations in VHF and global navigation satellite system (GNSS) signals, etc. (Tulasi Ram et al. 2008; Yadav et al. 2017; Aa et al. 2020). Among these, ionospheric scintillation is known to be a serious threat to transionospheric radio signals and is characterized by sudden, rapid, and irregular fluctuations of the amplitude and phase of the received signals due to the inhomogeneity in the electron density. Amplitude scintillations may cause the signal to fade and drop power below the threshold level of the tracking receiver, resulting in loss of data and cycle slips. Phase scintillation can cause frequency shifts in the received signals, which may exceed the phase lock loop bandwidth and result in a loss of phase lock (Aarons and Basu 1994). If sufficiently intense, the scintillation may profoundly affect the functional reliability and integrity of communications, surveillance, satellite, navigation, and augmentation systems, often exceeding the dynamic range of receivers leading to a complete loss of lock in the satellite link and may hold considerable time for reacquisition of the signal (Kintner et al. 2007). A complete outage of the signal leads to acute degradation of satellite-based communication and navigation systems services which may result in life-critical conditions in highly dynamic platforms such as aircraft's navigation and landing and threats to high-performance applications like maritime navigation, geophysical exploration, timekeeping, etc.

The consequence of scintillation is a serious threat to the receiver signal tracking performance of the L-band operated GNSS, which is the emerging satellite-based navigation system to replace the conventional ground-based navigation infrastructures in the aviation and maritime sectors. Usually, scintillations are more intense in the very high frequency (VHF) band than in the frequencies above 1 GHz, but under rare circumstances, the amplitude scintillations in the L band (1.575 GHz) could be more intense than that in the VHF band (251 MHz) (Bhattacharyya et al. 2017). It has been observed that the occurrence of loss-of-lock and cycle slips for all the GPS L band frequencies are more frequent when scintillation index $S4 \geq 0.6$ with a majority of the cycle slips of duration more than 6 s, whereas the modernized GPS L5 signal seems to be robust with minimal cycle slip durations (Biswas et al. 2019). Based on the relationship between the severity of phase scintillation and signal frequency, Moraes et al. (2017) pointed out a contradictory statement mentioning that the new civil signals L2C and L5 are more susceptible to the effects of the ionospheric scintillation in low latitudes. Nevertheless, scintillation has been a perplexity to the space science community and a significant challenge for the global and regional navigation satellite systems (GNSS & RNSS) and Satellite-based Augmentation System (SBAS) designers today (Roy and Paul 2013; Ratnam et al. 2018). Hence, the scintillation technique provides an integral measure of fluctuations in the phase and amplitude of the radio signals across a broad range of frequencies while passing through the ionosphere (Basu and Basu 1981).

The morphology of scintillations has been investigated and demonstrated for different parts of the globe, confirming its predominant occurrence in the equatorial ionization anomaly (EIA) region approximately extending across $\pm 15°$ to $\pm 20°$ of the magnetic equator, and in the auroral and polar cap regions using global observations and supported on theoretical grounds (Aarons 1982; Kil et al. 2002; Kintner et al. 2007; Nishioka et al. 2008; Huang 2018). From the global morphology of scintillations during solar maximum years, Aarons (1982) reported higher amplitudes of scintillations at equatorial ionization anomaly (EIA) crest latitudes. The strong scintillations over EIA and its onset time delay with respect to the magnetic equator in the South American sector have been presented by Kil et al. (2002). Kintner et al. (2007) suggested that although prominent occurrences of scintillations are often seen near the magnetic equator, they can appear at other latitudes irrespective of phases of the solar cycle. The characteristics of scintillations in the low and high-latitude regions are quite different due to the dissimilar mechanism of the processes (Knight 2000). Auroral and polar cap scintillations occur mainly due to the geomagnetic storms caused by an earthward directed coronal mass ejection (CME) associated with the solar flares and do not show any specific diurnal variation pattern and duration of occurrence. However, equatorial scintillations are relatively frequent and predominantly occur during the post-sunset hours, produced by the irregularities created by instabilities in the F-layer that disappear soon after midnight. Equatorial scintillations are pronounced during the equinoctial seasons and solar maximum period presenting a strong seasonal and solar activity dependence though such perception may not be true at all longitudes (Basu et al. 2002; Vyas and Dayanandan 2011; Kumar and Chen 2016; Tulasi Ram et al. 2017).

The primary condition responsible for nighttime equatorial scintillation is the pronounced Rayleigh–Taylor instability in the F-layer by rapid recombination at its lower part that leads to steep density gradients with the low-density plasma bubbles rising upwards (Ossakow 1981). The low-density bubbles eventually form into irregularity patches

and are guided along the magnetic field lines to manifest much stronger scintillation effects over the anomaly crest region ($\pm 15°$ to $\pm 20°$ dip latitudes) in both hemispheres than at the magnetic equator (Groves et al. 1997). The daytime scintillation, however is less frequent and most visible at mid-latitudes due to irregularity in the E region, popularly known as sporadic-E (Joshi et al. 2019). These are much less common and less predictable than nighttime equatorial scintillation by the F-layer processes (Fayose 2018).

In the last five decades, there have been extensive studies on ionospheric scintillations at several locations under various space weather science research programs (Koster 1972; Basu and Basu 1981; Tulasi Ram et al. 2006a). The characteristics of scintillations have been explored to some extent using regional as well as global scintillation data and employing closely spaced scintillation monitoring GNSS/VHF receivers (Mendillo et al. 1992; Bhattacharyya et al. 2001; Kil et al. 2002; Kintner et al. 2004; Burke et al. 2004; Otsuka et al. 2006; Dubey et al. 2006; Alfonsi et al. 2013). Bhattacharyya et al. (2001) found the signatures of irregularity in drift velocity structures being associated with plasma bubbles. Otsuka et al. (2006) explained the scintillation causing plasma irregularity through equinoctial asymmetry of the drift velocity. The depletions in TEC with the increase of the S4 index to manifest scintillations are attributed to the density irregularities by different researchers across South American, Indian and African regions (Dashora and Pandey 2005; Seemala and Valladares 2011). Several review articles on ionospheric scintillations and their various aspects and features have been demonstrated based on instrument observations, numerical and modelling practices (Koster 1972; Moorthy et al. 1979; Basu and Basu 1981; Rastogi et al. 1981a; Aarons 1982, 1985; Pathak et al. 1995; Basu et al. 2002; Singh et al. 2004; Tulasi Ram et al. 2006a; DasGupta et al. 2006). Rastogi et al. (1981b) explained the scintillations associated with geomagnetic activity through the modifications of electric fields at the equator. Tulasi Ram et al. (2006b) reported the threshold values of post-sunset vertical drifts at the equator during high and low solar activity years for the onset of intense scintillations at the EIA region.

In India, individual and coordinated scintillation studies have been done at various locations to understand the mechanism and diurnal as well as seasonal behavior of scintillations at varying scales (Somayajulu et al. 1977; DasGupta et al. 1981; Sastri 1984; Chandra 1990; Dabas et al. 1992; Jayachandran et al. 1993; Vyas 1994; Rama Rao et al. 1997; Chakraborty et al. 1999; Kumar and Gwal 2000; Singh et al. 2004). Their results explain the development mechanism of irregularities at the magnetic equator, its controlled field-aligned transfer, and the distinctly different nature of scintillations between the equator and anomaly crest. In brief, some systematic studies on various characteristics of diurnal, monthly, seasonal, or solar activity dependence of nighttime ionospheric scintillations have been carried out with limited campaign mode and long-term observations (Janve et al. 1979; Somayajulu et al. 1984; Dabas et al. 1992; Jayachandran et al. 1993; Balan et al. 1994; Kumar and Gwal 2000; Conker et al. 2003; Vyas and Dayanandan 2011; Omondi et al. 2019). There are some recent works on the occurrence and strength of scintillations through multi-frequency and multi-GNSS observations in the southern part of India concerning seasonal and solar conditions (Srinivasu et al. 2019). A latitudinal study of L-band scintillations associated with plasma irregularities has been conducted by Sripathi et al. (2018) using ionosonde and GPS observations, demonstrating the strength of scintillations with solar and geomagnetic indices. Sahithi et al. (2019) analyzed the scintillation occurrences and their variations at two low-latitude stations during a high solar active year in 2013. They demonstrated that the probability of occurrence is relatively higher during March equinox and December solstice, whereas the lowest occurrence rate was observed during June solstice. Paul et al. (2020) conducted a multi-wavelength coordinated observation, reporting irregularities at the poleward latitudes of the EIA crest even during solar minimum years. Goswami et al. (2022) reported the presence of post-midnight irregularities of different scale lengths around the EIA crest using multi-frequency observations. A systematic study of scintillations has been presented over Indian low-latitude location to improve understanding of the dynamics of plasma irregularities during the low solar activity period (Ayyagari et al. 2022). In brief, scintillation and associated phenomena have been a research topic of interest in the last two decades concerning the improvement in the understanding of underlying complex physical mechanisms and significant impacts on transionospheric propagation for communication and navigational applications.

Usually, the signal loss due to scintillation is attributed to either interference or failure of the equipment at the receiver/transmitter site by missing a nested robust model to account for the effects (Basu et al. 2002). Although a few climatological models have been developed, they are meant for planning purposes only. The support for space-based communication and navigation can be sensibly improved through an appropriate real-time specification and forecast model, enabling users to be aware of the occurrence well in advance and may instead employ alternate strategies to mitigate the effects (Basu et al. 2002; Ratnam et al. 2018; Sivavaraprasad et al. 2019). Attempts have been made with a few techniques to predict, detect and mitigate scintillations associated with EPBs, but they have not succeeded in providing reliable precursors and lack precision in explaining short-term discrepancies (Raghunath and Ratnam 2015; Ratnam et al. 2015; Priyadarshi 2015; Tadivaka et al. 2017;

Sivavaraprasad et al. 2019). There is still a lack of a comprehensive understanding of the underlying processes responsible for triggering EPBs (Narayanan et al. 2012).

Concerning the ionosphere over the region, the navigational solution across a significant part of the landmass is prone to scintillation threats being sandwiched between the magnetic equator and anomaly crest. Hence, it is essential to further probe the scintillation climatology through a chain of receivers extending from the equator to the outer edge of low latitude for understanding the scintillation statistics which would help in underlying the generation mechanism, loss of lock statistics and thereby developing the model for forecasting of scintillations over the region (Sridhar et al. 2017). Although there exists few modern customized scintillation monitoring GNSS systems in both amplitude and phase, their number is scarce as compared to the worldwide network of high-quality geodetic GNSS observing reference systems. It has been established that the low-resolution S4 index extracted from the signal-to-noise ratio from the traditional geodetic GNSS receivers could be used for the long-term amplitude scintillations analysis over any region in the case of inaccessibility to high sampling frequency scintillation monitoring receivers (Olwendo and Cilliers 2018; Mulugeta and Kassa 2022). Furthermore, it is essential to understand the scintillation occurrences with respect to time of the day, season, and solar activity at varying latitudes which may add to the knowledge of the different mechanisms of irregularity developments and their effectiveness over the region.

In the present study, we investigate the plasma irregularities and likely underlying mechanisms from a latitudinal array of locations extending from the near equator to the low-middle latitude transition region during the period from 2014 to 2017 that represents the descending phase of 24th solar cycle. Unlike specialized GNSS scintillation and TEC monitoring receivers, relatively coarser resolution amplitude scintillation index (S4) derived from the signal-to-noise ratio observables of traditional geodetic GNSS receivers are utilized in this study. Although it is possible to instead look at the Rate of Change of the TEC Index (ROTI) which is often used as a proxy for ionospheric scintillation with acceptable correlation with S4 index, the level of correlation may vary with latitudes depending on the associated scale length of irregularities (Ghimire et al. 2021; Kapil et al. 2022). ROTI is relatively more sensitive to the large-scale fluctuations in the ionosphere, with the scale size varying above a few kilometers, whereas the S4 index is sensitive to the small-to-medium scale irregularities with an order of a few hundred meters though these often coexist in the equatorial irregularity structures in the post unset hours (Basu et al. 1999; Yang and Liu 2016; Alfonsi et al. 2021; Vankadara et al. 2022). The key consideration in ROTI calculation is however based on the sharpness of the GNSS phase fluctuations due to the ionospheric irregularities for which it is most closely related to the phase scintillation. At this moment, we concentrate on the low-resolution amplitude scintillation index (S4), which could be supplemented by the high-resolution scintillation monitoring GNSS receivers' S4 observations in future.

The occurrences of post-sunset and post-midnight plasma irregularities and the probabilities of their seasonal occurrence are discussed through the variation of S4 amplitude in this study to improve the understanding of spatiotemporal ionospheric irregularities over the region. Finally, the occurrence frequency percentage of scintillations with respect to solar and geomagnetic indices are analyzed to infer the spatiotemporal characteristics of scintillations over the longitude sector.

## Materials and methods

In this study, we investigated the amplitude scintillation characteristics (S4 index) from GPS observations at three different locations arranged latitudinally from the magnetic equator to the outer edge of the average anomaly crest region. The geographic locations of the stations on the map are shown in Fig. 1 and their coordinate details along with the receiver descriptions are given in Table 1. The geomagnetic coordinates of the stations for the year 2017 are obtained from the World Data Center for Geomagnetism (http://wdc.kugi.kyoto-u.ac.jp/igrf/gggm/; accessed on 17 July 2021). It is notable from Fig. 1 that among the three stations considered in this study; one is situated at a near-equatorial location Bangalore (IISC) while the other two stations are situated at a beyond anomaly crest location (Lucknow; LCK4) and a far-low latitude location close to midlatitude (Jomsom; JMSM), respectively. IISC and LCK4 provide GPS observation data in receiver independent exchange (RINEX) format at a sampling rate of 30-sec, whereas that of JMSM is 15-sec. The RINEX observation data along with the broadcast ephemeris files and satellite differential code biases (DCBs) are processed through the GPS-TEC analysis application developed by Gopi Krishna Seemala at Institute for Scientific Research, Boston College, Boston, U.S.A. which can be accessed from his webpage at (https://seemala.blogspot.com; accessed on 11 March 2021) (Seemala and Valladares 2011). The receiver and interchannel biases are estimated by the program by minimizing the least squares. The S4 index is determined through the normalized root mean square (RMS) deviation of the detrended time series of signal-to-noise ratio (S/N) values in RINEX observations as given in Eq. 1. Similar studies have also been conducted by Sahithi et al. (Sahithi et al. 2019),

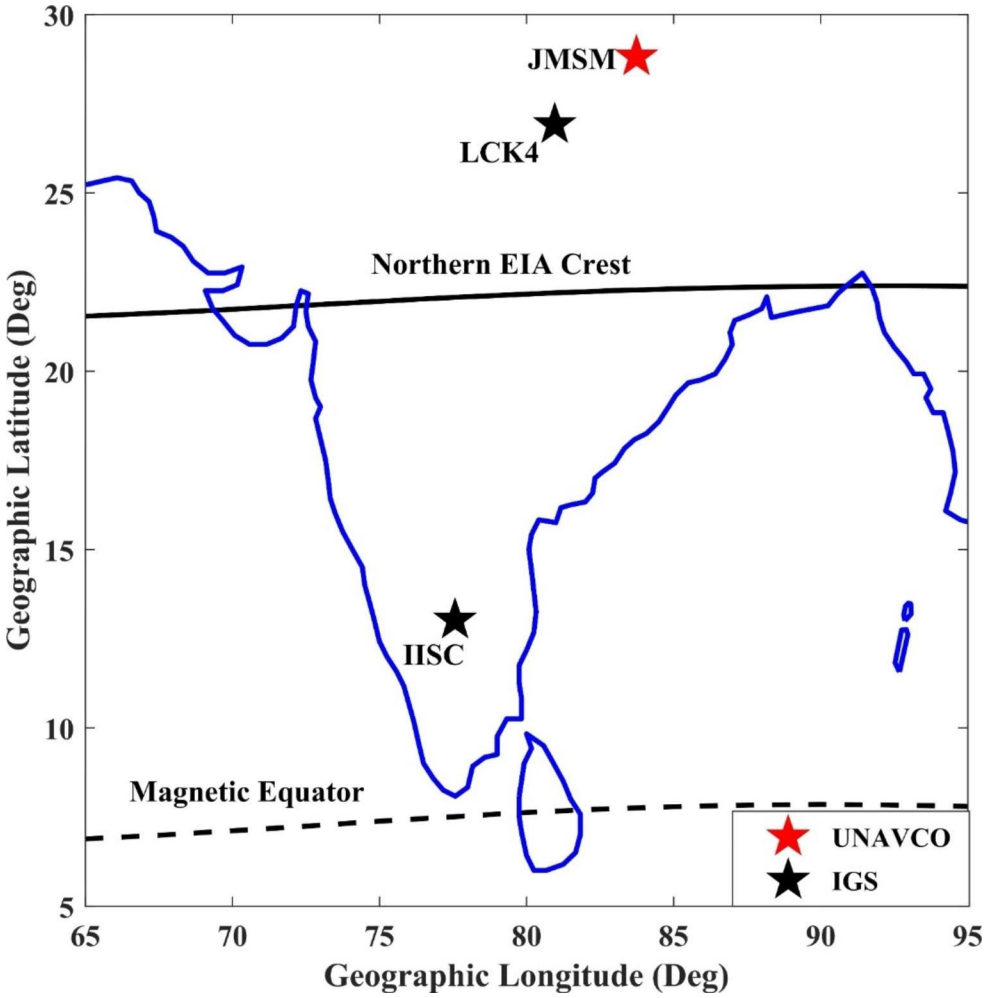


**Fig. 1** Geographical locations of Indian geodetic GNSS stations considered in the study for investigating scintillation occurrences. The dashed black contours represent the approximate locations of the magnetic equator, and the solid black contours represent the average position of northern equatorial ionization anomaly crest (EIA) latitudes across the Indian sector. The stations with black star symbol are under the IGS network whereas those with red star symbol are established under the UNAVCO network

**Table 1** List of the GNSS stations under IGS/UNAVCO network used to analyze amplitude scintillation index along with their name, station code, geographic and geomagnetic coordinates, and receiver descriptions

| S. No. | Station Code (Location) | Geog. Lat. in °N | Geog. Lon. in °E | Geom. Lat. in °N | Geom. Lon. in °E | GNSS Network/Receiver model and Antenna type | Data sampling rate |
|---|---|---|---|---|---|---|---|
| 1. | IISC (Bangalore, India) | 13.02 | 77.57 | 04.51 | 150.93 | IGS/ ASHTECH UZ-12, Choke ring | 30 s |
| 2. | LCK4 (Lucknow, India) | 26.91 | 80.96 | 18.11 | 155.31 | IGS/ LEICA GRX1200+GNSS, Choke ring | 30 s |
| 3. | JMSM (Jomsom, Nepal) | 28.81 | 83.74 | 19.82 | 158.05 | UNAVCO/ TRIMBLE NETRS, Choke ring | 15 s |

Ghimire et al. (Ghimire et al. 2021), and Dutta et al. (Dutta et al. 2018) by extracting S4 indices from geodetic GPS observables in the Indian and Nepal region, respectively. A comparative study of S4 recorded by dedicated scintillation monitoring receivers and those derived from IGS network data suggests that the S4 derived from IGS stations could be used at the regions having no dedicated scintillation receivers (Olwendo and Cilliers 2018; Mulugeta and Kassa 2022). The sampling interval of the S4 index extracted from IISC and LCK4 is 5-min whereas that of JMSM is 2.5-min, depending on the input temporal resolution of observables.

$$S4 = \sqrt{\frac{(< I^2 > - < I >^2)}{< I >^2}} \quad (1)$$

Where "*I*" is the detrended S/N parameters recorded along with the pseudorange and phase observables at the GPS station. The detailed procedure for extracting S4 parameters from the S/N observables are explicitly mentioned in articles in the past (Yeh and Liu 1982; Olwendo and Cilliers 2018; Luo et al. 2020; Atabati et al. 2021). It should be noted that there is no difference in the technique used to obtain the S4

index except the amplitude replaced by the S/N at a lower sampling rate in geodetic receivers.

The variability of the S4 index at the considered stations is investigated during the period from 2014 to 2017. While analyzing the quiet-time diurnal and seasonal climatology of the S4 index, the geomagnetically disturbed days with the geomagnetic Ap index above the quiet-time threshold ($\sum Ap > 24$) are eliminated. Furthermore, to understand the occurrence frequency of scintillations with respect to solar and geomagnetic activity levels, the S4 index frequency is plotted along with the monthly mean sunspot number (SSN), solar radio flux (F10.7), and Ap index which can be obtained from the OMNI Web-NASA server (https://omniweb.gsfc.nasa.gov/form/dx1.html; accessed on 17 July 2021).

The quantitative analysis of the scintillation data is performed by dividing the amplitude scintillation intensity into four levels following the classification scheme used by Goswami et al. (2020) and Xiong et al. (2007). Accordingly, S4 values below the threshold of 0.2 are not considered as scintillation events in this study. The four levels of S4 classifications are no scintillation ($S4 < 0.2$), weak ($0.2 < S4 \leq 0.4$), moderate ($0.4 < S4 \leq 0.6$), and strong ($S4 > 0.6$). Furthermore, to explore the scintillation characteristics effectively, an elevation cutoff of 30° has been applied, discarding the occurrences from the scintillation data which are possibly affected by the multipath effect. The diurnal variation of S4 indices at each location is plotted with respect to time in universal time (UT) as well as local time (LT = UT + 5:30 h) to understand the local time variability. To analyze the seasonal variation of the percentage of occurrence of scintillations, each year is divided into three seasons: equinox (March, April, September, and October), winter (November, December, January, and February,), summer (May, June, July, and August).

## Results and discussion

In Fig. 2, we show the variation of amplitude scintillation index (S4) with respect to universal time (UT) at (a) IISC, (b) LCK4, and (c) JMSM. The figure illustrates the general behavior of the ionospheric scintillations over the stations. The nighttime scintillations are generally associated with the occurrence of plasma bubbles due to Rayleigh-Taylor or $E \times B$ instability on the bottom side of the F-layer (Otsuka 2018; Abdu 2019). However, the daytime scintillations are associated with the blanketing sporadic E (Esb) layer, which is relatively less frequent and milder than the nighttime scintillations (Seif et al. 2015). From our observation, the scintillations were predominantly occurring between 14:00 to 20:00 UT at each station, corresponding to the local post-sunset and nighttime periods. The important observation from Fig. 2 is that while the IISC station (closer to the deep geomagnetic equator) observed intense post-midnight scintillations even greater than the post-sunset (pre-midnight), the LCK4 and JMSM, which are beyond anomaly crest location, did not display the post-midnight observations. Past reports show evidences of greater post-midnight ionospheric irregularities than the pre-midnight (pot-sunset) ionospheric irregularities over the equatorial region (Miller et al. 2010; Li et al. 2011; Dao et al. 2011; Otsuka et al. 2012; Yizengaw et al. 2013; Seba et al. 2021, 2022). The post-sunset scintillation activities have been extensively studied and are well explained by the Rayleigh-Taylor instability mechanism associated with the pre-reversal enhancement.

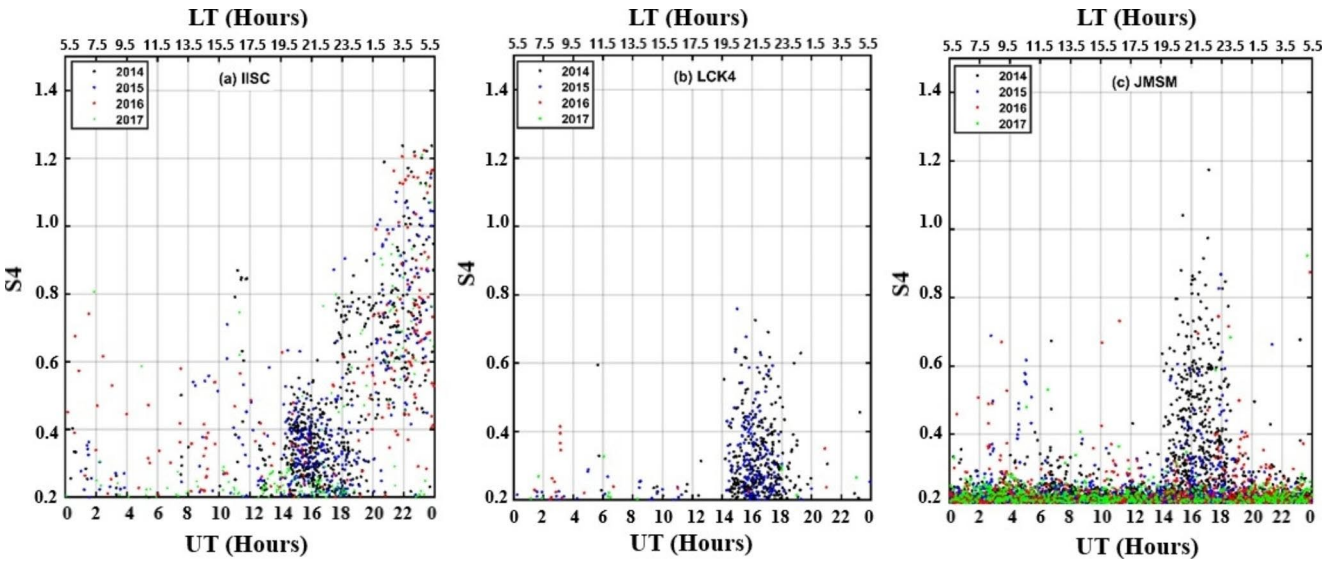


**Fig. 2** Variation of amplitude scintillation indices ($S4 > 0.2$) at (**a**) Bangalore (IISC), (**b**) Lucknow (LCK4), and (**c**) Jomsom (JMSM) during 2014 to 2017. The bottomside and topside X-axes represent the time in UT and LT, respectively

However, the measurement of intense post-midnight scintillation greater than the pre-midnight as well as the origin of the eastward electric field to develop Rayleigh-Taylor instability after local midnight are not well understood (Li et al. 2011; Otsuka 2018). However, the possible causes of enhanced eastward electric field could be associated with E region neutral wind dynamo, atmospheric gravity waves (AGWs), sporadic *E* layers development (Es), F layer uplift-ment by the meridional neutral winds, medium scale travelling ionospheric disturbances (MSTIDs), etc. (Yizengaw et al. 2013; Otsuka 2018; Seba et al. 2021) Furthermore, it has been reported that the occurrence peak of pre-midnight bubbles falls around equinox with the occurrence rate increasing during high solar activity, whereas the post-midnight bubbles are more frequent around summer solstice with the occurrence rate decreasing during high solar activity. As the overall solar activity in the solar cycle 24 is relatively lesser than the previous solar cycles, the aspect of dependance of plasma bubble occurrence on solar activity is not clearly discernable in our study. A high-rate sampling analysis of

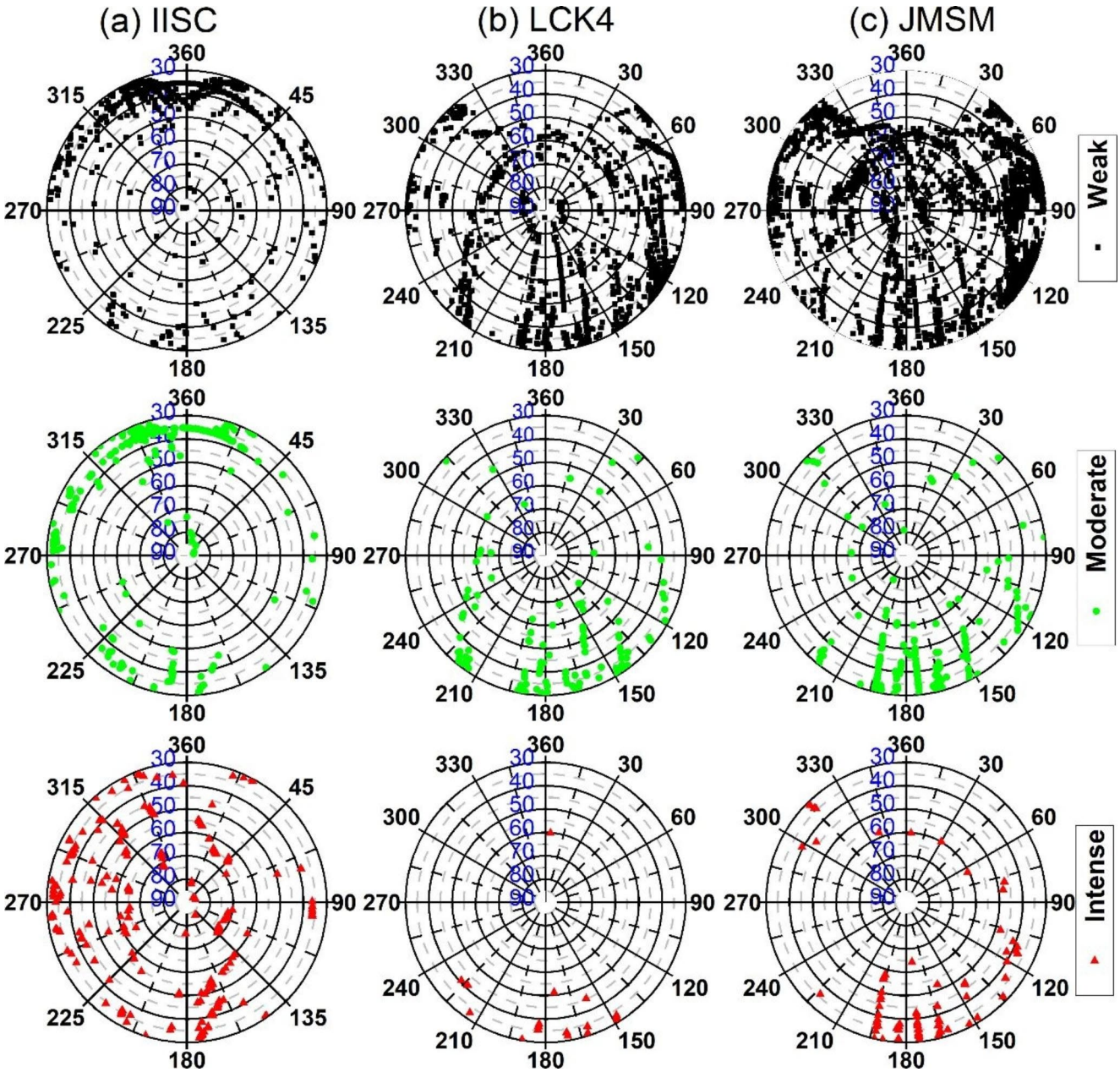


**Fig. 3** Directional distribution of amplitude scintillation indices of different levels in scattered sky plots at (**a**) Bangalore (IISC), (**b**) Lucknow (LCK4), and (**c**) Jomsom (JMSM) during 2014 to 2017. The top panels show weak scintillations whereas the middle and bottom panels are corresponding to moderate and intense scintillations, respectively. The concentric rings in the figures are elevation angles and the radial lines represent the azimuth directions of scintillation data points

S4 observations may provide a clear picture of this specific context. Moreover, evidence of post-midnight irregularities over the Indian sector during the June solstice of solar minimum has been presented earlier (Patra et al. 2009; Srinivasu et al. 2018; Aa et al. 2020; Goswami et al. 2022).

Among the years, the highest S4 value above the threshold (S4 > 0.2) at IISC is 0.742 in the year 2017 (low solar activity year), while the highest S4 value at the station is 1.237 in the year 2014 (high solar activity year). At LCK4, the maximum S4 value above the threshold is 0.304 in the year 2016 and 0.865 in the year 2014. For the JMSM station, the peak S4 value above the threshold is 0.659 which occurred in 2016, while the peak S4 value in 2015 was around 1.265.

It can be observed from Fig. 2 that the S4 values at LCK4 station are generally much lower than those at the IISC and JMSM stations. It should be noted that IISC is in the vicinity of the equatorial ionization anomaly (EIA) region and relatively nearer to the magnetic equator, making the irregularity development mechanism different from the other two beyond EIA crest locations (LCK4 and JMSM). The post-sunset irregularity across the EIA region is relatively stronger and more frequent during the equinox and winter solstice with the maxima generally observed around the EIA crest, depending on the strength of dusk time pre-reversal enhancement (PRE). On the contrary, the occurrence of post-midnight irregularity is relatively abundant during the June solstice, relying on the equatorward thermospheric wind (Aarons 1982). The effect of PRE is however minimal at LCK4, resulting in lesser S4 values than IISC (Rama Rao et al. 2006; Balan et al. 2018; Vankadara et al. 2022). The different distributions are due to two reasons: (a) the relatively high sampling data rate at JMSM and (b) the latitudinal location of JMSM seems to be following the low-mid latitude transition region behavior where the irregularities are weak but could be more frequent. This is mostly due to the associated medium-scale travelling ionospheric disturbances (MSTIDs) through Perkins instability, the neutral wind and electrical fields through sporadic E (Es) layer instability (Perkins 1973; Liu et al. 2021).

The daytime S4 values with amplitudes S4 > 0.2 are presumed to be scintillations whose development mechanisms are quite different from that of the post-sunset and post-midnight scintillations. Such occurrences are predominantly associated with the appearance of sporadic E (Es) causing a plasma gradient instability and can result in strong ionospheric scintillations even in the GNSS L-band frequency range. The favorable condition for the development of Es structure arises during a minimal electric field when the zonal wind facilitates metallic ions to converge to an altitude that can be transported towards the equator by the meridional wind. The higher occurrence of Es in the Indian sector has been earlier reported in the literature (Rastogi et al. 1977; Patel et al. 2009; Seif et al. 2015; Uma et al. 2018). Moreover, strong amplitude scintillations at each of the stations occurred between 2014 and 2015, while the lowest values occurred in 2016 and 2017, demonstrating the solar activity dependence of the scintillation occurrences. The stronger post-sunset scintillations during high solar activity years refer to the much larger amplitude of PRE and perturbation of the background electron density due to enhanced solar activity (Deng et al. 2013).

Figure 3 shows the overall directional distribution of weak (top panel), moderate (middle panel) and intense (bottom panel) amplitude scintillation indices of different levels in scattered sky plots at (a) IISC, (b) LCK4, and (c) JMSM during the period from 2014 to 2017. The distribution of S4 measurements over the locations is mainly based on the latitude and longitudinal location of observation, footprints of the GPS PRNs at the given elevation cut-off, the occurrence of scintillations with respect to local solar time and the sampling rate of the receiver observation (Jiao et al. 2013; Abadi et al. 2014). From the first observation, it can be noticed that the scintillation patches are denser at lower elevation angles which is more conspicuous for weak and moderate scintillations, leading to increased probability of loss of scenarios as discussed in earlier reports (Skone et al. 2001; Tran et al. 2017; Srinivasu et al. 2022). It is clear from the figure that the number of intense scintillations is high at the near-equatorial station (IISC), whereas weak scintillations are high in number at the far-low latitude station (JMSM). It should be noted that the analysis is undertaken based on the samples captured through the satellite footprints over the region; however, it is likely that there are regions not in the coverage of the PRNs the scintillations over which cannot be accounted in the statistical analysis, which is the drawbacks of such satellite-based analysis. Hence, with the available datasets the analysis is performed in this study. Furthermore, it can be observed from the scattered sky plots that the occurrence location of moderate and intense plots at IISC is randomly distributed as opposed to their apparent occurrence distributions in the southward directions at LCK4 and JMSM. In brief, the occurrence of intense scintillation seems to be more prevalent within the EIA region, while weak scintillations very often find themselves at a large density in the far low latitude stations adjacent to middle latitude. This supports the explanation provided for the observation in Fig. 2, presenting maximum occurrences of post-sunset plasma irregularities across the EIA region during equinox and winter solstices and that of post-midnight irregularities during summer solstice which are relatively sparse at LCK4 and JMSM as they are situated far away in the outer side of EIA crest. The large density of weaker

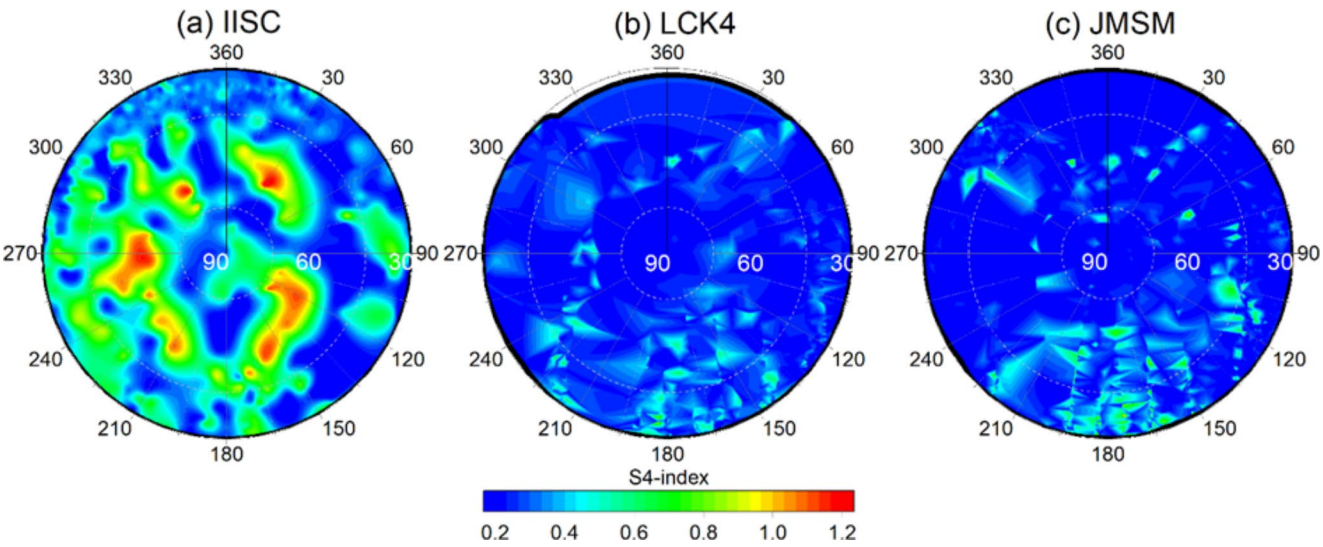


**Fig. 4** The 2-dimensional surface sky plots of scintillation amplitudes at (**a**) Bangalore (IISC), (**b**) Lucknow (LCK4), and (**c**) Jomsom (JMSM) during 2014 to 2017

scintillations at farther latitudes corresponds to the frequent participation of MSTID and Es instability.

The 2-dimensional surface sky plot of scintillation amplitudes at each station is presented in Fig. 4. At IISC, the distribution is almost symmetrical along the east-west direction but concentrated in the northern sky of IISC. Most of the scintillations occur within 315° to 45° azimuth and at 30° elevation angle. Also, intense scintillations are observed almost at every elevation angle at this location. LCK4 and JMSM show a different situation from IISC; the scintillation distribution is concentrated in the southern sky (equator-ward) and eastward of LCK4 and JMSM (pole-ward). No scintillations were observed between 330° to 30° azimuth with the elevation cut off below 50°. The intense scintillations at both stations were observed mostly between 30° to 50° elevation angles. From the 2-dimensional surface sky plots of scintillation amplitudes from 2014 to 2017 shown in Fig. 4, it is evident that the maximum scintillation amplitudes occur at IISC at elevation angles greater than 50°. These high amplitudes occur at each of the azimuthal quadrants of IISC. Only weak and moderate scintillation amplitudes are observed at LCK4 and JMSM and

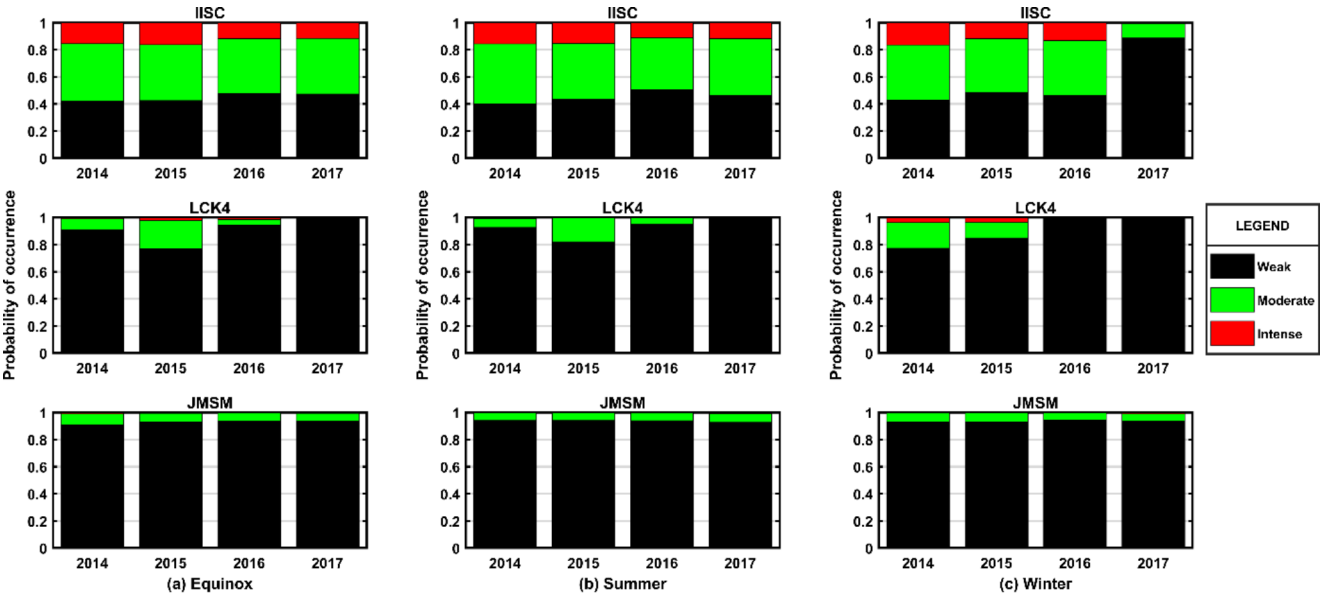


**Fig. 5** Seasonal probability of occurrence of amplitude scintillations at Bangalore (IISC), Lucknow (LCK4), and Jomsom (JMSM) during 2014 to 2017. The seasons are classified as equinox (February, March, April, August, September, and October), summer (May, June, and July) and winter (November, December, and January) for all the years under consideration and plotted all together. The probability of occurrence of scintillations with black, green, and red color represent the weak, moderate and intense scintillations, respectively

predominantly between 30° to 50° elevation angles and at 120° to 230° (south-east) in azimuth. It should be mentioned that the whole analysis is based on the samples captured by the PRN footprints which is not practically distributed evenly across the region and intrinsically depends on the availability of the signals over any regions. The observed variation pattern is in accordance with the frequency of occurrence of plasma irregularities in the EIA region (IISC) and beyond (LCK4 and JMSM) in the northern hemisphere. The post-sunset irregularities are evidently with maximum amplitudes around the EIA crest, primarily associated with the Rayleigh–Taylor instability in the F-layer beyond which the amplitudes decrease with a different mechanism of instability for irregularity development towards middle latitudes (Perkins 1973; Aarons 1982; Liu et al. 2021; Goswami et al. 2022). Moreover, the high frequency of weak irregularities at the poleward side of the EIA crest and its highest occurrence around JMSM is attributed to the significant role of MSTID and Es occurrences over the latitudinal sector.

In order to understand the seasonal variability of the amplitude scintillations, the probability of occurrence of amplitude scintillations at each station in a year, we determined the normalized by the number of occurrences corresponding to the total number of observations. Figure 5 shows the probability of occurrence of amplitude scintillations in the equinox, summer, and winter seasons at the three selected stations from 2014 to 2017. The probability of occurrence of scintillations is categorized into weak, moderate, and intense levels and plotted for all the seasons. From the very first observation from Fig. 5, it can be marked that, irrespective of scintillation magnitudes, the highest probability of occurrence of scintillation is observed at the JMSM station, followed by the IISC station, while the minimum percentage of occurrence is observed at the LCK4 station. At the equatorial IISC station, the occurrence of weak, moderate, and intense scintillations is noticed in all the seasons. The maximum occurrence of intense scintillation at this station is observed during the high solar active equinox (2014 and 2015), followed by the winter solstice whereas the summer solstice witnesses maximum occurrences of intense scintillations during high and moderate to low solar activity years (2015 to 2017). At LCK4 and JMSM, the percentage of occurrence of intense scintillation is very minimal during equinox and hardly seen in other seasons. At LCK4, intense scintillations are sparsely observed in the equinox of 2014. The occurrences of moderate scintillations are relatively maximum at LCK4 whereas that of weak scintillations is observed to be maximum at JMSM.

It is clear from the figure that at JMSM the intense and moderate scintillations only occurred during the high solar active equinox season (2014 and 2015) whereas the equinox seasons under moderate to low solar activity and both summer and winter realize the sole occurrence of weak scintillations. The existence of irregularities well beyond the EIA crest in the Indian region during the low solar activity year has been reported by Paul et al. (2020). In brief, the percentage occurrence of scintillations is highest in the high solar active equinox seasons at all the stations, followed by the winter season, while the lowest percentage occurrence of scintillations occurs during the summer season over each of the stations. Concerning latitudinal variability of scintillation amplitudes, maximum intense scintillation occurrences are primarily restricted to near-equatorial IISC whereas moderate and weak scintillation occurrences adhere to the far low latitude station JMSM and beyond anomaly crest station LCK4, respectively. The seasonal and solar activity dependence of post-sunset and post-midnight irregularities including that of the sparsely observed daytime irregularities with respect to latitudinal locations are the drivers for the variations in the probability of occurrences of scintillations over the region.

To further realize the frequency of amplitude scintillation occurrences during diverse solar and geomagnetic conditions, we plotted the monthly amplitude scintillation frequency with the monthly solar (SSN and F10.7) and geomagnetic indices (Ap) at all the three-station during the period from 2014 to 2017 as shown in Fig. 6. It is observed that moderate and intense scintillations occur more in the year 2014 and 2015 which correspond to the period of high solar activity in the 24th solar cycle. The occurrence of intense scintillations gradually decreases towards moderate to low solar activity years during 2016 and 2017. Thus, the variation in intense scintillation occurrence depends on the variation in solar activity. A close observation of Fig. 6 also reveals that the S4 seasonal variation indicates high scintillation frequencies are observed during the equinox and winter seasons as compared to the summer season. The monthly scintillation frequency plots at individual stations also demonstrate that the scintillation activity over the stations changes monthly, seasonally, and with solar activity levels. Moreover, we did not observe a definite relationship with the geomagnetic Ap index in our study. The correlation analysis of scintillation indices with the solar activity and geomagnetic indices have been performed in the past which confirms that although there is evidence of acceptable correlation of scintillation indices with solar and geomagnetic indices, the dependency is not true very often as it may vary with latitudes depending on the associated scale length of irregularities. Although the scintillation occurrences were found to vary linearly with solar activity it could be either triggered or suppressed depending on the local electrodynamics (Kumar et al. 2016). The effect of solar activity is again influenced by seasonal variations. This suggests that there are different impacts of solar activity, geomagnetic

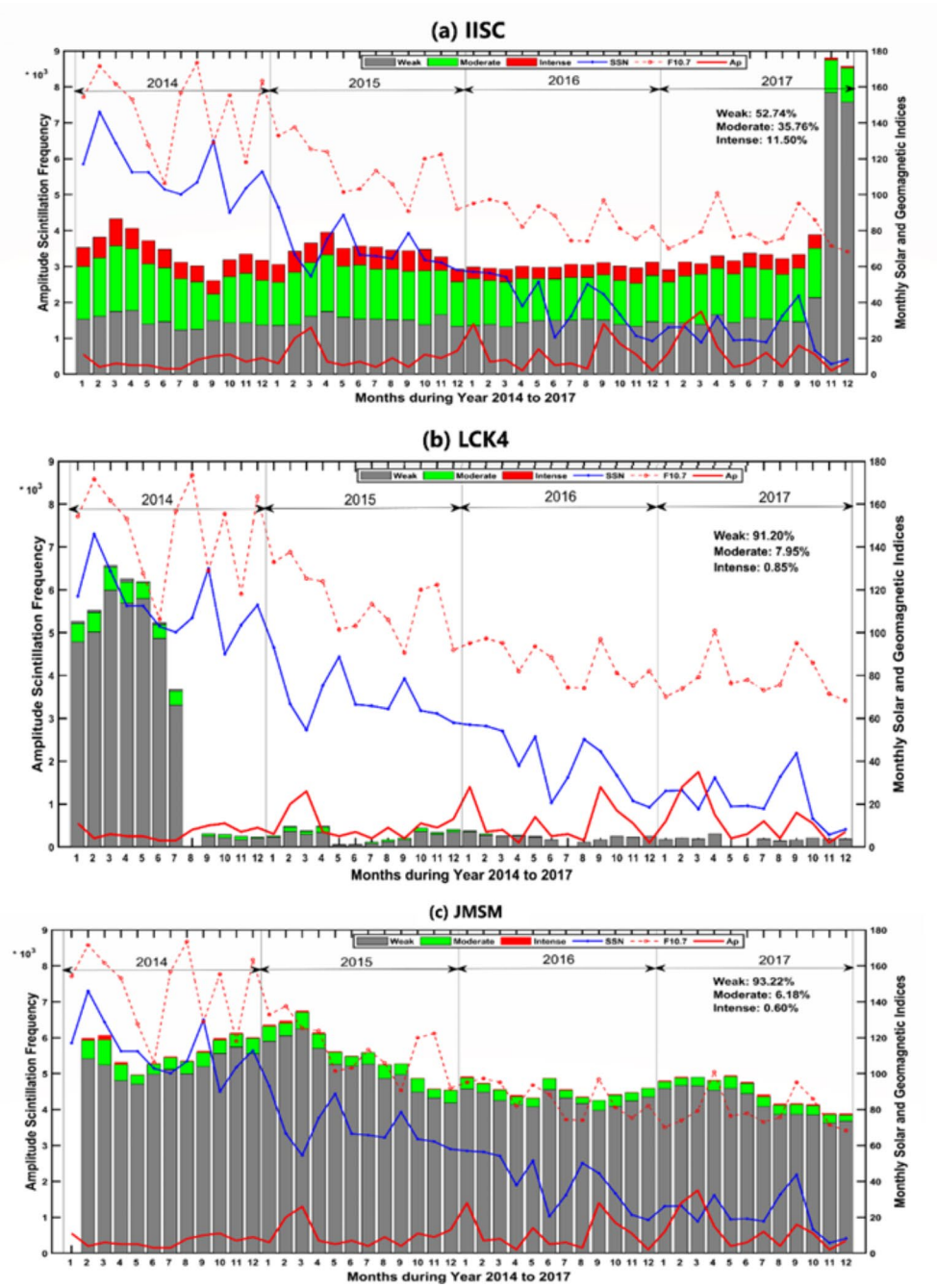


**Fig. 6** Variation of monthly Amplitude scintillation frequencies at (**a**) Bangalore (IISC), (**b**) Lucknow (LCK4), and (**c**) Jomsom (JMSM) along with the monthly variation of solar (SSN and F10.7) and geomagnetic (Ap) indices during 2014 to 2017. The weak, moderate, and intense scintillation frequencies are represented with gray, green, and red colors, respectively

activity, and seasons on scintillation in different geographic locations (Jiao and Morton 2015). Among all the locations, the highest percentage of scintillation frequency is noticed at IISC (11.50%), followed by LCK4 (0.85%) and JMSM (0.60%). The respective percentage of occurrence frequencies for moderate (35.76%, 7.95%, and 6.18%) and weak (52.74%, 91.20%, and 93.22%) scintillations are also realized for stations arranged with respect to the departure from the magnetic equator. Moreover, the drop in amplitude scintillation frequency at LCK4 starting from half of 2014 could be attributed to the subdued extent of the low latitude scintillation effects to the station latitude during the low solar activity period in the 24th solar cycle. We ascribe the sudden increased weak scintillation amplitude frequency at the end of 2017 due to the low vertical plasma drifts during the post-sunset F-layer in this period. The results agree with the lowest equatorial plasma bubbles (EPBs) occurrences in 2017, reported by Chaurasia et al. (2022) using Defense Meteorological Satellite Program (DMSP) observations over the region during the period from 2014 to 2017. The sudden jump in amplitude scintillation frequency could also

be due to time dependent failures/issues of the receiving stations.

We further looked at the correlation coefficients between the scintillation index (S4) and the solar and geomagnetic indices at each station, as shown in Table 2. Looking at the correlations between S4 occurrence rate and SSN, we observe that at IISC, there is a weak negative correlation between S4 occurrence rate and SSN (r=-0.15). This indicates that the scintillation index decreases slightly as the sunspot number increases. At LCK4, on the other hand, there is a moderate positive correlation between S4 occurrence rate and SSN (r = 0.55), indicating that as the sunspot number increases, the S4 occurrence rate also increases. The same trend is observed at JMSM, where a moderate positive correlation exists between S4 occurrence rate and SSN (r = 0.48). We can conclude that the correlation between S4 occurrence rate and SSN is stronger at LCK4 and JMSM compared to IISC. In contrast, the direction of the correlation is opposite at IISC compared to the other two stations. Next, we looked at the correlations between S4 occurrence rate and Ap. At IISC, there is a weak negative correlation the occurrence rate and Ap (r=-0.05), indicating that as the Ap index increases, the scintillation index occurrence rate decreases slightly. At LCK4, the correlation between S4 occurrence rate and Ap is also weak and negative (r=-0.16), suggesting a slight decrease in the occurrence rate as the Ap index increases. At JMSM, however, the correlation between S4 occurrence rate and Ap is almost negligible (r = 0.005). Therefore, we can conclude that the correlation between S4 occurrence rate and Ap is weak and negative at all three stations, with the strongest correlation at LCK4. Finally, we analyzed the correlations between S4 occurrence rate and F10. At IISC, there is a weak negative correlation between S4 occurrence rate and F10 (r=-0.11), indicating that the scintillation occurrence rate decreases slightly as the F10 solar index increases. At LCK4, there is a moderate positive correlation between S4 occurrence rate and F10 (r = 0.38), indicating that as the F10 solar index increases, the scintillation index occurrence rate also increases moderately. At JMSM, there is a strong positive correlation between S4 occurrence rate and F10 (r = 0.51), indicating that the occurrence rate increases significantly as the F10 solar index increases. Therefore, we can conclude that the correlation between S4 occurrence rate and F10 is moderate to strong at all three stations, with the strongest correlation at JMSM. In brief, our results show that the correlation is moderate for the LCK4 and JMSM stations, which are beyond the north anomaly crest location, but for the station closer to geomagnetic latitude, IISC, it is found to be weak that contradicts with earlier studies that demonstrates that the irregularities occurrence rates in any regions had a good correlation with F10.7 (Nishioka et al. 2008; Li et al. 2020; Kuai et al. 2022). However, there are also instances of results with long terms observations showing lesser or negative correlation coefficients between the irregularities occurrence rate and the F10.7 at the deep equatorial latitudes (Huang et al. 2014; Aa et al. 2020; Nguyen Thanh et al. 2021). Moreover, (2020) suggested that the EPB occurrence rate could be more strongly correlated with the F10.7 index on an annual basis than on a monthly basis.

**Table 2** Correlation coefficients between S4 occurrence rate with solar and geomagnetic indices

| S4 occurrence rate/Station | SSN | Ap | F10 |
|---|---|---|---|
| IISC (Bangalore, India) | -0.14564 | -0.054 | -0.10964 |
| LCK4 (Lucknow, India) | 0.550185 | -0.16276 | 0.375454 |
| JMSM (Jomsom, Nepal) | 0.481479 | 0.004729 | 0.50887 |

In general, we have observed that the correlation coefficients between S4 occurrence rate with the solar and geomagnetic indices (SSN, Ap, and F10) at the GNSS stations (IISC, LCK4, and JMSM) vary in strength and direction. The correlation between S4 occurrence rate and SSN is stronger at LCK4 and JMSM compared to IISC, while the correlation with Ap is weak and negative at all three stations. The correlation with F10 is moderate to strong at all three stations, with the strongest correlation at JMSM. These results highlight the importance of studying the relationships between solar and geomagnetic indices and scintillation index at different locations, as the correlations can vary significantly depending on the specific solar index and location. This information can be helpful in predicting and mitigating the impact of space weather on GNSS systems, as scintillation can cause errors and interruptions in GNSS signals.

The vital importance of such analysis of scintillation occurrences over the Indian longitude sector is important owing to its geomagnetic location in the equatorial and low latitude sector which is more prone to scintillation occurrences and governed by the underlying equatorial electrodynamics, wind, and temperature dynamics. It should be noted that the large-scale phenomena associated with the TEC are understood to a greater extent and mitigated through the regional and global ionosphere maps (RIM and GIM), Indian Regional Navigation Satellite System (IRNSS), GPS Aided GEO Augmented Navigation (GAGAN) over the Indian region. However, addressing the abnormalities and loss of lock scenarios in the satellite-based navigation receivers due to the scintillation occurrences is a crucial aspect among researchers as well as navigation engineers as it may lead to severe threats in highly dynamic environments. Hence, there are scopes for investigating the spatiotemporal climatology of scintillation indices over the equatorial and low-latitude Indian region for effective mitigation of the scintillation effects in the signals of operational instruments.

## Summary and conclusions

In this paper, ionospheric amplitude scintillation indices are investigated over the Indian longitude sector from three selected latitudinally aligned geodetic quality GPS observations under the IGS and UNAVCO network during the period from 2014 to 2017, referring to the descending phase of the 24th solar cycle. The S4 index extracted from the GPS observations was used to study the temporal and spatial characteristics of the amplitude scintillation index at near-equatorial (Bangalore; IISC), beyond northern anomaly crest (Lucknow; LCK4), and far low latitude station close to the middle latitudes (Jomsom; JMSM) in the Indian longitude sector. The higher scintillations were predominantly observed between post-sunset and nighttime periods over each station, manifesting a more significant occurrence of post-sunset irregularities than in other parts of the day. Strong amplitude scintillations at each of the stations occurred between 2014 and 2015, while the lowest values occurred in 2016 and 2017 that describing the solar activity dependence of the scintillation occurrences. The relatively lower amplitude of scintillations at LCK4 than at IISC and JMSM indicates that the EIA crest might be falling at closer latitudes during the study period. The scattered directional distribution of amplitude scintillation indices confirms intense scintillation occurrence being more prevalent at near-equatorial locations while most of the scintillation occurrences are weak at the higher low latitude stations. This supports the plasma instability and irregularities development mechanism and scintillation strengths around the low-middle latitude transition regions (mostly weak) than the EIA region (moderate to strong). The occurrence locations of moderate and intense scintillations are randomly distributed at IISC with a higher concentration of scintillation distribution in the poleward direction as opposed to the southward distributions of the scintillation occurrences at LCK4 and JMSM. Furthermore, the probability of occurrence of scintillations is seen to be maximum in the high solar active equinox seasons at all the stations, followed by the winter season while the minimum percentage occurrence of scintillations occurs during the summer season at each of the stations. The findings demonstrate that the magnitude and orientation of the correlation between the S4 occurrence rate with solar and geomagnetic indices can differ considerably depending on the particular solar index and GNSS station. However, it is realized that there are different impacts of solar activity, geomagnetic activity, and seasons on scintillation in different geographic locations.

Nevertheless, it is also realized that the scintillation activity over the latitudinal range of locations changes diurnally, monthly, seasonally, and with the solar activity level which is of major concern for the space-based navigation and positioning applications over the region as the reliability, accuracy, and availability may be severely affected due to the resulted cyclic slips and loss of locks in the receivers. The analysis drawn from the amplitude scintillation observations in this study adds to the efforts for forecasting and eventually mitigating the scintillation effects in the navigation and positioning solutions. With the recent advancement of satellite-based navigation mass market and establishment of the autonomous IRNSS and GAGAN, the major perpetrator of the post-sunset degraded performance of the receivers is now established as the scintillations due to plasma bubble occurrences in the low latitude sector. Hence, in the present work the scintillation levels, occurrence frequencies, and distributions with respect to spatial and temporal scale have been discussed with the S4 index for understanding its variability over the region. Further analysis of scintillation and loss of lock events from the recently established specialized GNSS ionospheric scintillation and TEC monitoring (GISTM) station at KL University, Guntur, Andhra Pradesh that lies in the EIA region is the subsequent objective of this research work.

**Acknowledgements** S.K.P. acknowledge Koneru Lakshmaiah Education Foundation for providing necessary laboratory space for conducting this research work. The authors appreciate Gopi K. Seemala for obtaining the GPS-TEC analysis program to extract the S4 index from the GPS observables.

**Author contributions** Conceptualization, S.K.P.; methodology, S.K.P. and M.M.; software, S.K.P., M.M. and K.A.; validation, S.K.P., M.M., J.W. and K.A.; formal analysis, S.K.P., M.M., J.W. and K.A.; investigation, S.K.P. and M.M.; resources, S.K.P.; data curation, S.K.P.; writing—original draft preparation, S.K.P. and M.M.; writing—review and editing, S.K.P., M.M., J.W. and K.A.; visualization, S.K.P., M.M., J.W. and K.A.; project administration, S.K.P.; funding acquisition, S.K.P.

**Funding** This research was funded by the Core Research Grant (CRG) scheme under the Science & Engineering Research Board (SERB) (A statutory body of the Department of Science & Technology, Government of India) New Delhi, India under grant number CRG/2019/003394. The research was also partially funded by the Warsaw University of Technology within the Excellence Initiative: Research University (IDUB) program.

**Data Availability** The authors acknowledge the UNAVCO Data Center (ftp://data-out.unavco.org/pub/rinex/; accessed on 28 August 2021) the Crustal Dynamics Data Information System (CDDIS) archive (https://cddis.nasa.gov/archive/gnss/, accessed on 12 September 2021). for providing access to the GNSS observation data used in this study. The solar and geomagnetic data used in this study are obtained from the NASA-OMNI archives (https://omniweb.gsfc.nasa.gov/; accessed on 17 July 2021).

## Declarations

**Institutional review board statement** Not applicable.

**Informed consent** Not applicable.

**Conflict of interest** The authors declare no conflict of interest. The funders had no role in the design of the study; in the collection, analyses, or interpretation of data; in the writing of the manuscript, or in the decision to publish the results.



## References

Aa E, Zou S, Liu S (2020) Statistical analysis of equatorial plasma irregularities retrieved from Swarm 2013–2019 observations. J Geophys Research: Space Phys 125. https://doi.org/10.1029/2019JA027022. :e2019JA027022

Aarons J (1982) Global morphology of ionospheric scintillations. Proc IEEE 70:360–378. https://doi.org/10.1109/PROC.1982.12314

Aarons J (1985) Construction of a model of equatorial scintillation intensity. Radio Sci 20:397–402. https://doi.org/10.1029/RS020i003p00397

Aarons J, Basu S (1994) Ionospheric amplitude and phase fluctuations at the GPS frequencies. pp 1569–1578

Abadi P, Saito S, Srigutomo W (2014) Low-latitude scintillation occurrences around the equatorial anomaly crest over Indonesia. Ann Geophys 32:7–17. https://doi.org/10.5194/angeo-32-7-2014

Abdu MA (2019) Day-to-day and short-term variabilities in the equatorial plasma bubble/spread F irregularity seeding and development. Progress in Earth and Planetary Science 6:11. https://doi.org/10.1186/s40645-019-0258-1

Alfonsi L, Spogli L, Pezzopane M et al (2013) Comparative analysis of spread-F signature and GPS scintillation occurrences at Tucumán, Argentina. J Geophys Research: Space Phys 118:4483–4502. https://doi.org/10.1002/jgra.50378

Alfonsi L, Cesaroni C, Spogli L et al (2021) Ionospheric disturbances over the indian Sector during 8 September 2017 geomagnetic storm: plasma structuring and propagation. Space Weather 19. https://doi.org/10.1029/2020SW002607. e2020SW002607

Atabati A, Alizadeh M, Schuh H, Tsai L-C (2021) Ionospheric scintillation prediction on S4 and ROTI parameters using Artificial neural network and genetic algorithm. Remote Sens 13. https://doi.org/10.3390/rs13112092

Ayyagari D, Datta A, Chakraborty S (2022) Systematic study of ionospheric scintillation over the indian low-latitudes during low solar activity conditions. Adv Space Res. https://doi.org/10.1016/j.asr.2022.07.026

Balan N, Bailey GJ, Nair RB, Titheridge JE (1994) Nighttime enhancements in ionospheric electron content in the northern and southern hemispheres. J Atmos Terr Phys 56:67–79. https://doi.org/10.1016/0021-9169(94)90177-5

Balan N, Liu L, Le H (2018) A brief review of equatorial ionization anomaly and ionospheric irregularities. Earth and Planetary Physics 2:257–275. https://doi.org/10.26464/epp2018025

Basu S, Basu S (1981) Equatorial scintillations—a review. J Atmos Terr Phys 43:473–489. https://doi.org/10.1016/0021-9169(81)90110-0

Basu S, Groves KM, Quinn JM, Doherty P (1999) A comparison of TEC fluctuations and scintillations at Ascension Island. J Atmos Solar Terr Phys 61:1219–1226. https://doi.org/10.1016/S1364-6826(99)00052-8

Basu S, Groves KM, Basu Su, Sultan PJ (2002) Specification and forecasting of scintillations in communication/navigation links: current status and future plans. J Atmos Solar Terr Phys 64:1745–1754. https://doi.org/10.1016/S1364-6826(02)00124-4

Bhattacharyya A, Basu S, Groves KM et al (2001) Dynamics of equatorial F region irregularities from spaced receiver scintillation observations. Geophys Res Lett 28:119–122. https://doi.org/10.1029/2000GL012288

Bhattacharyya A, Kakad B, Gurram P et al (2017) Development of intermediate-scale structure at different altitudes within an equatorial plasma bubble: implications for L-band scintillations. J Geophys Research: Space Phys 122:1015–1030. https://doi.org/10.1002/2016JA023478

Biswas T, Ghosh S, Paul A, Sarkar S (2019) Interfrequency Performance Characterizations of GPS during Signal Outages from an Anomaly Crest Location. Space Weather 17:803–815. https://doi.org/10.1029/2018SW002105

Burke WJ, Gentile LC, Huang CY et al (2004) Longitudinal variability of equatorial plasma bubbles observed by DMSP and ROCSAT-1. J Geophys Research: Space Phys 109:A12301. https://doi.org/10.1029/2004JA010583

Chakraborty SK, DasGupta A, Ray S, Banerjee S (1999) Long-term observations of VHF scintillation and total electron content near the crest of the equatorial anomaly in the indian longitude zone. Radio Sci 34:241–255. https://doi.org/10.1029/98RS02576

Chandra H (1990) Equatorial spread-F-Recent developments. Ind J Radio Space Phys 19:215–224

Chaurasiya SK, Patel K, Singh AK (2022) Equatorial plasma bubbles for solar maximum & moderate year of the solar cycle 24. Adv Space Res 70:2856–2866. https://doi.org/10.1016/j.asr.2022.07.036

Conker RS, El-Arini MB, Hegarty CJ, Hsiao T (2003) Modeling the effects of ionospheric scintillation on GPS/Satellite-Based Augmentation System availability. Radio Sci 38:1001. https://doi.org/10.1029/2000RS002604

Dabas RS, Banerjee PK, Bhattacharya S et al (1992) Study of equatorial plasma bubble dynamics using GHz scintillation observations in the indian sector. J Atmos Terr Phys 54:893–901. https://doi.org/10.1016/0021-9169(92)90056-Q

Dao E, Kelley MC, Roddy P et al (2011) Longitudinal and seasonal dependence of nighttime equatorial plasma density irregularities during solar minimum detected on the C/NOFS satellite. Geophys Res Lett 38. https://doi.org/10.1029/2011GL047046

DasGupta A, Maitra A, Basu S (1981) Occurrence of nighttime VHF scintillations near the equatorial anomaly crest in the indian sector. Radio Sci 16:1455–1458. https://doi.org/10.1029/RS016i006p01455

DasGupta A, Paul A, Ray S et al (2006) Equatorial bubbles as observed with GPS measurements over Pune, India. Radio Sci 41. https://doi.org/10.1029/2005RS003359. RS5S28

Dashora N, Pandey R (2005) Observations in equatorial anomaly region of total electron content enhancements and depletions. Ann Geophys 23:2449–2456. https://doi.org/10.5194/angeo-23-2449-2005

Deng B, Huang J, Liu W et al (2013) GPS scintillation and TEC depletion near the northern crest of equatorial anomaly over South

China. Adv Space Res 51:356–365. https://doi.org/10.1016/j.asr.2012.09.008
Dubey S, Wahi R, Gwal AK (2006) Ionospheric effects on GPS positioning. Adv Space Res 38:2478–2484. https://doi.org/10.1016/j.asr.2005.07.030
Dutta B, Kalita BR, Bhuyan PK et al (2018) Spatial features of L-Band Equinoctial Scintillations from Equator to Low Midlatitude at around 95°E during 2015–2016. J Geophys Research: Space Phys 123:7767–7788. https://doi.org/10.1029/2018JA025533
Fayose RS (2018) Investigation of Ionosphere Scintillations variability over azure; a terrestrial point within the equatorial Anomaly Region. IOSR J Appl Phys (IOSR-JAP) 50–55. https://doi.org/10.9790/4861-1003035055
Ghimire BD, Chapagain NP, Khadka B et al (2021) GPS TEC scintillations and TEC depletion as seen from Hetauda and NAST, Nepal for 2016. BIBECHANA 18:87–94. https://doi.org/10.3126/bibechana.v18i2.33405
Goswami S, Ray S, Paul A (2020) Degradation of Satellite-Based Navigation Performance observed from an Anomaly Crest Location in the indian Longitude Sector. Radio Sci 55. https://doi.org/10.1029/2019RS007042. e2019RS007042
Goswami S, Ghosh S, Paul A (2022) Multifrequency observations of Postmidnight Ionospheric irregularities from an Anomaly Crest Location. Radio Sci 57. https://doi.org/10.1029/2022RS007437. :e2022RS007437
Groves KM, Basu S, Weber EJ et al (1997) Equatorial scintillation and systems support. Radio Sci 32:2047–2064. https://doi.org/10.1029/97RS00836
Huang C-S (2018) Effects of the postsunset vertical plasma drift on the generation of equatorial spread F. Progress in Earth and Planetary Science 5:3. https://doi.org/10.1186/s40645-017-0155-4
Huang C-S, de La Beaujardiere O, Roddy PA et al (2014) Occurrence probability and amplitude of equatorial ionospheric irregularities associated with plasma bubbles during low and moderate solar activities (2008–2012). J Geophys Research: Space Phys 119:1186–1199. https://doi.org/10.1002/2013JA019212
Janve AV, Rai RK, Deshpande MR et al (1979) On the nighttime enhancements in ionospheric total content at low latitudes. Ann de Geophysique 35:159–165. http://inis.iaea.org/search/search.aspx?orig_q=RN:11525036
Jayachandran B, Balan N, Rao PB et al (1993) HF Doppler and ionosonde observations on the onset conditions of equatorial spread F. J Geophys Research: Space Phys 98:13741–13750. https://doi.org/10.1029/93JA00302
Jiao Y, Morton YT (2015) Comparison of the effect of high-latitude and equatorial ionospheric scintillation on GPS signals during the maximum of solar cycle 24. Radio Sci 50:886–903. https://doi.org/10.1002/2015RS005719
Jiao Y, Morton YT, Taylor S, Pelgrum W (2013) Characterization of high-latitude ionospheric scintillation of GPS signals. Radio Sci 48:698–708. https://doi.org/10.1002/2013RS005259
Joshi LM, Tsai L-C, Su S-Y et al (2019) VHF Scintillation and Drift studied using Spaced Receivers in Southern Taiwan. Radio Sci 54:455–467. https://doi.org/10.1029/2018RS006722
Kapil C, Seemala GK, Shetti DJ, Acharya R (2022) Reckoning ionospheric scintillation S4 from ROTI over indian region. Adv Space Res 69:915–925. https://doi.org/10.1016/j.asr.2021.10.026
Kil H, Kintner PM, de Paula ER, Kantor IJ (2002) Latitudinal variations of scintillation activity and zonal plasma drifts in South America. Radio Sci 37:1006. https://doi.org/10.1029/2001RS002468
Kintner PM, Ledvina BM, de Paula ER, Kantor IJ (2004) Size, shape, orientation, speed, and duration of GPS equatorial anomaly scintillations. Radio Sci 39:1–23. https://doi.org/10.1029/2003RS002878
Kintner PM, Ledvina BM, de Paula ER (2007) GPS and ionospheric scintillations. Space Weather 5:S09003. https://doi.org/10.1029/2006SW000260
Knight MF (2000) Ionospheric Scintillation Effects on Global Positioning System Receivers. PhD Thesis, The University of Adelaide, Australia 297–304. https://hdl.handle.net/2440/19809
Koster JR (1972) Equatorial scintillation. Planet Space Sci 20:1999–2014. https://doi.org/10.1016/0032-0633(72)90056-6
Kuai J, Wang K, Zhong J et al (2022) Analysis of the ionospheric irregularities and phase scintillation at low and middle latitudes based on Swarm Observations. Remote Sens 14. https://doi.org/10.3390/rs14194780
Kumar S, Chen W (2016) Remote sensing of ionospheric plasma bubbles using GPS/GNSS. In: 2016 International Conference on Localization and GNSS (ICL-GNSS). pp 1–5
Kumar S, Gwal AK (2000) VHF ionospheric scintillations near the equatorial anomaly crest: solar and magnetic activity effects. J Atmos Solar Terr Phys 62:157–167. https://doi.org/10.1016/S1364-6826(99)00090-5
Kumar S, Chen W, Liu Z, Ji S (2016) Effects of solar and geomagnetic activity on the occurrence of equatorial plasma bubbles over Hong Kong. J Geophys Research: Space Phys 121:9164–9178. https://doi.org/10.1002/2016JA022873
Li G, Ning B, Abdu MA et al (2011) On the occurrence of postmidnight equatorial F region irregularities during the June solstice. J Geophys Research: Space Phys 116. https://doi.org/10.1029/2010JA016056
Li Q, Zhu Y, Fang K, Fang J (2020) Statistical study of the Seasonal Variations in TEC depletion and the ROTI during 2013–2019 over Hong Kong. Sens (Basel) 20. https://doi.org/10.3390/s20216200
Liu Y, Zhou C, Xu T et al (2021) Review of ionospheric irregularities and ionospheric electrodynamic coupling in the middle latitude region. Earth and Planetary Physics 5:eepp2021025. https://doi.org/10.26464/epp2021025
Luo X, Gu S, Lou Y et al (2020) Amplitude scintillation index derived from C/N0 measurements released by common geodetic GNSS receivers operating at 1 hz. J Geodesy 94:27. https://doi.org/10.1007/s00190-020-01359-7
Mendillo M, Baumgardner J, Pi X et al (1992) Onset conditions for equatorial spread F. J Geophys Research: Space Phys 97:13865–13876. https://doi.org/10.1029/92JA00647
Miller ES, Makela JJ, Groves KM et al (2010) Coordinated study of coherent radar backscatter and optical airglow depletions in the central Pacific. J Geophys Research: Space Phys. https://doi.org/10.1029/2009JA014946. 115:
Moorthy KK, Reddi CR, Murthy BVK (1979) Night-time ionospheric scintillations at the magnetic equator. J Atmos Terr Phys 41:123–134. https://doi.org/10.1016/0021-9169(79)90004-7
Moraes A, de O, Costa E, Abdu MA et al (2017) The variability of low-latitude ionospheric amplitude and phase scintillation detected by a triple-frequency GPS receiver. Radio Sci 52:439–460. https://doi.org/10.1002/2016RS006165
Mulugeta S, Kassa T (2022) Comparison of GPS loss of lock with S4-proxy from IGS network data and S4 from SCINDA network data over Bahir Dar. J Atmos Solar Terr Phys 229:105828. https://doi.org/10.1016/j.jastp.2022.105828
Narayanan VL, Taori A, Patra AK et al (2012) On the importance of wave-like structures in the occurrence of equatorial plasma bubbles: a case study. J Geophys Research: Space Phys 117:A01306. https://doi.org/10.1029/2011JA017054
Nguyen Thanh D, Le Huy M, Amory-Mazaudier C et al (2021) Characterization of ionospheric irregularities over Vietnam and adjacent region for the 2008–2018 period. Vietnam J Earth Sci 43:465–484. https://doi.org/10.15625/2615-9783/16502
Nishioka M, Saito A, Tsugawa T (2008) Occurrence characteristics of plasma bubble derived from global ground-based GPS receiver

networks. J Geophys Research: Space Phys 113:1–12. https://doi.org/10.1029/2007JA012605
Olwendo J, Cilliers P (2018) A comparison of ionospheric scintillation proxy indices derived from low rate IGS data with the amplitude scintillation index, S4, in a low latitude region over Africa. J Atmos Solar Terr Phys 173:160–167. https://doi.org/10.1016/j.jastp.2018.04.012
Omondi GE, Baki P, Ndinya BO (2019) Total electron content and scintillations over Maseno, Kenya, during high solar activity year. Acta Geophys 67:1661–1670. https://doi.org/10.1007/s11600-019-00354-7
Ossakow SL (1981) Spread-F theories—a review. J Atmos Terr Phys 43:437–452. https://doi.org/10.1016/0021-9169(81)90107-0
Otsuka Y (2018) Review of the generation mechanisms of post-midnight irregularities in the equatorial and low-latitude ionosphere. Progress in Earth and Planetary Science 5:57. https://doi.org/10.1186/s40645-018-0212-7
Otsuka Y, Shiokawa K, Ogawa T (2006) Equatorial Ionospheric Scintillations and Zonal Irregularity drifts observed with Closely-Spaced GPS Receivers in Indonesia. J Meteorol Soc Jpn 84A:343–351. https://doi.org/10.2151/jmsj.84A.343
Otsuka Y, Shiokawa K, Nishioka M (2012) VHF radar observations of post-midnight F-region field-aligned irregularities over Indonesia during solar minimum. Indian J Radio Space Phys 41:199–207
Patel K, Singh AK, Patel RP, Singh RP (2009) Characteristics of low latitude ionospheric E-region irregularities linked with daytime VHF scintillations measured from Varanasi. J Earth Syst Sci 118:721–732. https://doi.org/10.1007/s12040-009-0058-x
Pathak KN, Jivrajani RD, Joshi HP et al (1995) Study of ionospheric scintillations near the crest of equatorial anomaly in India using digital database. Indian J Radio Space Phys 24:138–150. https://cir.nii.ac.jp/crid/1571417125202064384
Patra AK, Phanikumar DV, Pant TK (2009) Gadanki radar observations of F region field-aligned irregularities during June solstice of solar minimum: first results and preliminary analysis. J Geophys Research: Space Phys 114:A12305. https://doi.org/10.1029/2009JA014437
Paul A, Sur D, Haralambous H (2020) Multi-wavelength coordinated observations of ionospheric irregularity structures from an anomaly crest location during unusual solar minimum of the 24th cycle. Adv Space Res 65:1402–1413. https://doi.org/10.1016/j.asr.2019.11.035
Perkins F (1973) Spread F and ionospheric currents. J Geophys Res (1896–1977) 78:218–226. https://doi.org/10.1029/JA078i001p00218
Priyadarshi S (2015) A review of Ionospheric Scintillation Models. Surv Geophys 36:295–324. https://doi.org/10.1007/s10712-015-9319-1
Raghunath S, Ratnam DV (2015) Detection of low-latitude ionospheric irregularities from GNSS Observations. IEEE J Sel Top Appl Earth Obs Remote Sens 8:5171–5176. https://doi.org/10.1109/JSTARS.2015.2496201
Rama Rao PVS, Jayachandran PT, Sri Ram P et al (1997) Characteristics of VHF radiowave scintillations over a solar cycle (1983–1993) at a low-latitude station: Waltair (17.7°N, 83.3°E). Ann Geophys 15:729–733. https://doi.org/10.1007/s00585-997-0729-3
Rama Rao PVS, Gopi Krishna S, Niranjan K, Prasad DSVVD (2006) Study of spatial and temporal characteristics of L-band scintillations over the indian low-latitude region and their possible effects on GPS navigation. Ann Geophys 24:1567–1580. https://doi.org/10.5194/angeo-24-1567-2006
Rastogi RG, Deshpande MR, Murthy BS, Davies K (1977) Daytime satellite radio scintillation and sporadic E near the magnetic equator. Geophys Res Lett 4:113–115. https://doi.org/10.1029/GL004i003p00113
Rastogi RG, Mullen JP, MacKenzie E (1981a) Effect of geomagnetic activity on equatorial radio VHF scintillations and spread F. J Geophys Research: Space Phys 86:3661–3664. https://doi.org/10.1029/JA086iA05p03661
Rastogi RG, Mullen JP, MacKenzie E (1981b) Effect of geomagnetic activity on equatorial radio VHF scintillations and spread F. J Geophys Research: Space Phys 86:3661–3664. https://doi.org/10.1029/JA086iA05p03661
Ratnam DV, Sivavaraprasad G, Lee J (2015) Automatic ionospheric scintillation detector for global navigation satellite system receivers. IET Radar Sonar Navig 9:702–711. https://doi.org/10.1049/iet-rsn.2014.0232
Ratnam DV, Dabbakuti JRKK, Lakshmi NVVNJS (2018) Improvement of Indian-Regional Klobuchar Ionospheric Model Parameters for single-frequency GNSS users. IEEE Geosci Remote Sens Lett 15:971–975. https://doi.org/10.1109/LGRS.2018.2827081
Roy B, Paul A (2013) Impact of space weather events on satellite-based navigation. Space Weather 11:680–686. https://doi.org/10.1002/2013SW001001
Sahithi K, Sridhar M, Kotamraju SK et al (2019) Characteristics of ionospheric scintillation climatology over indian low-latitude region during the 24th solar maximum period. Geod Geodyn 10:110–117. https://doi.org/10.1016/j.geog.2018.11.006
Sastri JH (1984) Duration of equatorial spread-F. Ann Geophys 2:353–358. http://hdl.handle.net/2248/3824
Seba EB, Nigussie M, Giday NM, Moldwin MB (2021) The relationship between Upward Propagating Atmospheric gravity waves and ionospheric irregularities during Solar Minimum Periods. Space Weather 19. https://doi.org/10.1029/2021SW002715.e2021SW002715
Seba EB, Nigussie M, Moldwin MB (2022) The role of global thermospheric zonal winds on the variability of equatorial ionospheric irregularities. J Atmos Solar Terr Phys 233–234:105873. https://doi.org/10.1016/j.jastp.2022.105873
Seemala GK, Valladares CE (2011) Statistics of total electron content depletions observed over the south american continent for the year 2008. Radio Sci 46:1–14. https://doi.org/10.1029/2011RS004722
Seif A, Tsunoda RT, Abdullah M, Hasbi AM (2015) Daytime gigahertz scintillations near magnetic equator: relationship to blanketing sporadic E and gradient-drift instability. Earth Planets and Space 67:177. https://doi.org/10.1186/s40623-015-0348-2
Singh RP, Patel RP, Singh AK (2004) Effect of solar and magnetic activity on VHF scintillations near the equatorial anomaly crest. Ann Geophys 22:2849–2860. https://doi.org/10.5194/angeo-22-2849-2004
Sivavaraprasad G, Venkata Ratnam D, Otsuka Y (2019) Multicomponent Analysis of Ionospheric Scintillation Effects using the Synchrosqueezing technique for monitoring and mitigating their impact on GNSS signals. J Navig 72:669–684. https://doi.org/10.1017/S0373463318000929
Skone S, Knudsen K, de Jong M (2001) Limitations in GPS receiver tracking performance under ionospheric scintillation conditions. Phys Chem Earth Part A 26:613–621. https://doi.org/10.1016/S1464-1895(01)00110-7
Somayajulu YV, Garg SC, Vijayakumar PN (1977) Scintillation studies using ATS-6 radio beacons at Delhi. Indian J Radio Space Phys 6:250–256. http://nopr.niscpr.res.in/handle/123456789/37459
Somayajulu YV, Garg SC, Dabas RS et al (1984) Multistation study of nighttime scintillations in low latitudes: evidence of control by equatorial F region irregularities. Radio Sci 19:707–718. https://doi.org/10.1029/RS019i003p00707
Sridhar M, Venkata Ratnam D, Padma Raju K et al (2017) Ionospheric scintillation forecasting model based on NN-PSO technique. Astrophys Space Sci 362. https://doi.org/10.1007/s10509-017-3144-6

Srinivasu VKD, Dashora N, Prasad DSVVD et al (2018) On the occurrence and strength of multi-frequency multi-GNSS ionospheric scintillations in indian sector during declining phase of solar cycle 24. Adv Space Res 61:1761–1775. https://doi.org/10.1016/j.asr.2017.08.036

Srinivasu VKD, Prasad DSVVD, Niranjan K et al (2019) L-band scintillation and TEC variations on St. Patrick's Day storm of 17 March 2015 over indian longitudes using GPS and GLONASS observations. J Earth Syst Sci 128:69. https://doi.org/10.1007/s12040-019-1097-6

Srinivasu VKD, Dashora N, Prasad DSVVD, Niranjan K (2022) Loss of lock on GNSS signals and its association with ionospheric irregularities observed over indian low latitudes. GPS Solutions 26:34. https://doi.org/10.1007/s10291-021-01218-8

Sripathi S, Sreekumar S, Banola S (2018) Characteristics of equatorial and low-latitude plasma irregularities as investigated using a Meridional Chain of Radio experiments over India. J Geophys Research: Space Phys 123:4364–4380. https://doi.org/10.1029/2017JA024980

Tadivaka RV, Paruchuri BP, Miriyala S et al (2017) Detection of ionospheric scintillation effects using LMD-DFA. Acta Geophys 65:777–784. https://doi.org/10.1007/s11600-017-0058-1

Tran TL, Le HM, Amory-Mazaudier C, Fleury R (2017) Climatology of ionospheric scintillation over the Vietnam low-latitude region for the period 2006–2014. Adv Space Res 60:1657–1669. https://doi.org/10.1016/j.asr.2017.05.005

Tulasi Ram S, Rama Rao PVS, Niranjan K et al (2006a) The role of post-sunset vertical drifts at the equator in predicting the onset of VHF scintillations during high and low sunspot activity years. Ann Geophys 24:1609–1616. https://doi.org/10.5194/angeo-24-1609-2006

Tulasi Ram S, Rama Rao PVS, Niranjan K et al (2006b) The role of post-sunset vertical drifts at the equator in predicting the onset of VHF scintillations during high and low sunspot activity years. Ann Geophys 24:1609–1616. https://doi.org/10.5194/angeo-24-1609-2006

Tulasi Ram S, Rama Rao PVS, Prasad DSVVD et al (2008) Local time dependent response of postsunset ESF during geomagnetic storms. J Geophys Research: Space Phys 113:A07310. https://doi.org/10.1029/2007JA012922

Tulasi Ram S, Ajith KK, Yokoyama T et al (2017) Vertical rise velocity of equatorial plasma bubbles estimated from equatorial atmosphere Radar (EAR) observations and HIRB model simulations. J Geophys Research: Space Phys 122:6584–6594. https://doi.org/10.1002/2017JA024260

Uma G, Brahmanandam PS, Srinivasu VKD et al (2018) Daytime VHF amplitude scintillations recorded at an indian low-latitude station, Waltair (17.7°N, 83.3°E) during 1997–2003. Adv Space Res 61:1736–1743. https://doi.org/10.1016/j.asr.2017.07.004

Vankadara RK, Panda SK, Amory-Mazaudier C et al (2022) Signatures of equatorial plasma bubbles and Ionospheric Scintillations from Magnetometer and GNSS Observations in the indian longitudes during the Space Weather events of early September 2017. https://doi.org/10.3390/rs14030652. Remote Sensing 14:

Vyas GD (1994) VHF scintillation and spread-F in the anomaly crest region. Ind J Radio Space Phys 23:157–164. http://nopr.niscpr.res.in/handle/123456789/35861

Vyas, Dayanandan B (2011) Study of night time VHF ionospheric scintillations near the crest of equatorial Appleton anomaly indian station, Udaipur (24.6°N, 73.7°E). Acta Geod et Geophys Hungarica 46:10–24. https://doi.org/10.1556/AGeod.46.2011.1.2

Xiong B, Wan W-X, Ning B-Q et al (2007) A comparison and analysis of the S4 index, C/N and roti over Sanya. Chin J Geophys 50:1414–1424. https://doi.org/10.1002/cjg2.1161

Yadav S, Sridharan R, Sunda S, Pant TK (2017) Further refinements to the spatiotemporal forecast model for L-band scintillation based on comparison with C/NOFS observations. J Geophys Research: Space Phys 122:5643–5652. https://doi.org/10.1002/2017JA023869

Yang Z, Liu Z (2016) Correlation between ROTI and ionospheric scintillation indices using Hong Kong low-latitude GPS data. GPS Solutions 20:815–824. https://doi.org/10.1007/s10291-015-0492-y

Yeh KC, Liu C-H (1982) Radio wave scintillations in the ionosphere. Proceedings of the IEEE 70:324–360

Yizengaw E, Retterer J, Pacheco EE et al (2013) Postmidnight bubbles and scintillations in the quiet-time June solstice. Geophys Res Lett 40:5592–5597. https://doi.org/10.1002/2013GL058307